Development of Damage Fragility Functions for URM Chimneys and Parapets

H. Krawinkler, 1940-2012
Stanford University, Stanford, California, U.S.A.

J.D. Osteraas, B.M. McDonald, & J.P. Hunt
Exponent – Failure Analysis Associates, Menlo Park, California, U.S.A.

SUMMARY:
Unreinforced masonry (URM) chimneys and parapets are common in many residential and commercial areas in California and elsewhere, and widespread failures routinely occur in any earthquake of significance. Given the extensive history of such failures, one might assume a plethora of empirical data which, combined with simple numerical models, could be readily used to develop fragility functions for these elements. A concerted effort to do just that proved the fallacy of that assumption. As part of the ATC-58 Project "Guidelines for Seismic Performance Assessment of Buildings", the authors developed fragility functions based on a combination of empirical data, hand calculations, and computer modeling. Simple, common failure mechanisms proved to be difficult to quantify and challenging to model. Ultimately, the paucity of consistent, hard data necessitated a heavy infusion of engineering judgment. Two primary damage states were identified for both URM chimneys and parapets: (1) cracking with residual offset (sliding) and (2) toppling. Several seismic intensity measures and engineering demand parameters were correlated to damage, and peak ground acceleration and peak (absolute) roof velocity were selected for the chimney and parapet fragility functions, respectively. Empirical datasets from post-earthquake surveys of chimneys and parapets provided a starting point in the development of the fragility functions. Incremental dynamic analyses were conducted using Working Model 2D to simulate chimney and parapet response using the far-field suite of ground motions developed for ATC-63 (FEMA P695). Intensities resulting in toppling or sliding were recorded and ranked to form fragility functions. Lognormal fragility functions were then developed to present the probability of sliding or toppling as a function of seismic intensity or engineering demand parameter. Recognizing the significant effect of building and diaphragm stiffness, fragility function parameters were developed as a function of building characteristics. While chimneys and parapets were the subject of this study, the methodology is widely applicable to the development of fragility functions for other non-structural components, equipment, and building contents.

Keywords: fragility function; unreinforced masonry; chimney; parapet

1. INTRODUCTION

Masonry chimneys and parapets are two of the most fragile building components. Virtually all post-earthquake reconnaissance reports mention significant numbers of damaged or toppled chimneys or parapets. For example, seven days after the 2010 Christchurch earthquake, it had been reported that 14,000 insurance claims involving chimney damage had been received, from a total of 50,000 claims (Newstalk ZB, 2010; Griffith *et al*., 2010). For the 1994 Northridge earthquake, City of Los Angeles records identify approximately 30,000 chimneys for which repair permits were issued while other sources report a total of 60,000 damaged chimneys (LADB&S, 1994). While these data reinforce the fragile nature of masonry chimneys/parapets, like most field data reviewed, there are no data on the number or construction details of chimneys/parapets that were undamaged. A number of studies do report the number of damaged as well as undamaged chimneys/parapets within a portion of the area affected by the earthquake, though the data sets are quite small, especially for higher intensities of ground shaking.

Unlike other building components which are generally standardized, construction of chimneys and parapets is typically based on regional practices and artistry of masons as opposed to standard designs, engineered or not. Areas of similar construction can exhibit not only a wide range of damage severity, but also a seemingly endless number of damage modes. As a consequence, the response of this seemingly simple component is in reality quite complicated: First, one cannot rely on the strength or ductility of key components such as mortar, wall or roof ties, reinforcing bond/development, etc. Second, the onset of substantial nonlinearity associated with first cracking and onset of rocking or sliding of all or part of the chimney/parapet can occur at low intensity and early in the ground shaking record. For instance, the restoring moment of a cracked, free-standing chimney/parapet acting as a rocking rigid block decreases as block rotation increases. In addition, incorporation of stiffness and strength degradation due to rocking, mortar crushing, damage to adjacent framing, etc., is difficult, at best, to model realistically.

2. EMPIRICAL DATA

Numerous chimney/parapet damage states have been observed following earthquakes, ranging from complete collapse to cracking that can only be identified by careful inspection. Available data sets contain little information on the nature of the chimney/parapet damage observed. Two common and reasonably well-defined damage states were selected for analysis: Damage State 1 (DS1) captures those conditions where damage would be readily apparent (i.e. visible cracking, sliding of the chimney/parapet), likely resulting in a Yellow Tag – Area Unsafe, and require removal or replacement of that portion above the crack. DS1 does not include damage that can only be identified with a detailed inspection of the chimney. Thus, subtle damage is not reflected in the statistics for DS1. Damage State 2 (DS2) captures all toppling damage that has potential for human injury. Examples of the two damage states are shown in Figure 1 and Figure 2 for chimneys and parapets, respectively.

Figure 1. Left: chimney sliding (Santa Rosa, M_w=5.6, 1969); right: toppling (San Fernando, M_w=6.6, 1971). Photo credits: nisee.berkeley.edu/elibrary/

2.1. Chimneys

As discussed above, while widely reported following every earthquake, there are few published post-event surveys that present chimney damage statistics in sufficient detail to provide a basis for development of fragility functions. Six such useful data sets have been utilized in this study.

Following the 1971 San Fernando earthquake, Scholl (1974) conducted damage surveys of 1,043 mostly residential buildings in two areas of the City of Glendale. Virtually all buildings surveyed were more than 20 years old and large percentages (69% and 84% in the two areas) were greater than 40 years old. Of those, 610 had chimneys, of which 212 were classified as damaged – the classification of "damage" was binary – no detail on the nature or extent of damage to chimneys (including fireplaces) was collected or reported.

Figure 2. Left: parapet sliding (Santa Rosa, M_w=5.6, 1969); right: toppling (Loma Prieta, M_w=6.9, 1989). Photo credits: nisee.berkeley.edu/elibrary/

For the 1994 Northridge earthquake, two sets of data on chimney damage are publically available. ATC-38 (1994) conducted a systematic survey of about 500 buildings located within 1,000 feet of 31 strong-motion recording stations; the dataset includes 233 buildings with chimneys of which 57 were identified with some degree of damage. In many cases, qualitative comments regarding the nature of chimney damage were included, though there is no apparent consistency between inspectors regarding chimney damage characterization. Selected ground motion data for the 31stations was presented in the report, while time history data and response spectra were contained on the CD. In addition, Graf (2009) assembled data from detailed inspections of 225 residential properties, 157 of which had chimneys. Roughly one-third of the chimneys were constructed before 1940.

While several reports on the 2001 Nisqually earthquake reference chimney damage, derivation of defensible fragility functions is difficult. Booth *et al*. (2004) conducted a systematic windshield survey (using binoculars) of approximately 60,000 chimneys over 50km^2 and identified 1,556 damaged chimneys. The objective of their survey was not to study chimney damage as such but to identify pockets of damage corresponding to geological features, using observed chimney damage as an indicator of shaking intensity. Data recorded for damaged chimneys consisted of GPS coordinates and three classes of damage (small cracks, large cracks/partial collapse, chimney partially or totally destroyed). The total number of chimneys in an area was determined from analysis of air photos. McMullin *et al*. (2001) surveyed 120 houses in an Olympia neighborhood just east of the capitol grounds. 84 chimneys were observed, of which 28 had visible damage.

Chimney performance data for the 2003 San Simeon earthquake were obtained from the California Earthquake Authority (CEA). The data set included 97 masonry chimneys on 90 dwellings, of which between 20 and 27 had reported damage. Entries for damaged chimneys also included their repair cost, though there is not information whether one or multiple chimneys at a dwelling were damaged. The data set also includes the site PGA derived from ShakeMap, year of construction and number of stories.

Given the large size of the Booth dataset for the Nisqually earthquake and concerns about the validity of the data, especially with respect to the denominators, both numerators and denominators in Booth's dataset were divided by 100 before entering into the combined dataset. A maximum likelihood curve fitting algorithm was provided by Baker and Zareian (2009). The solver routine weights each data point to accurately reflect the number of observations in the fitted log-normal curve. An additional number of undamaged chimneys, equal in number to 1,000 times the size of the dataset, was added to each dataset at a PGA of 0.05g to reflect the fact that a very high percentage of chimneys in areas of low PGA would not be damaged, but that non-damage data would not be reflected in any dataset because properties in areas of low ground shaking intensity were not surveyed. The addition of these "zero" data points has the effect of anchoring the fragility function close to zero probability of failure at very low PGAs. A logarithmic cumulative distribution with a median value of 0.39g PGA and a dispersion of 0.5 was the best fit through the combined data sets. All of the above data are plotted in Figure 3 (left) along with the fitted fragility function.

2.2. Parapets

Empirical data on damage to parapet walls in masonry buildings were obtained from field reports from the 1989 Loma Prieta earthquake (Lizundia *et al*., 1991) and 1994 Northridge earthquake (Lizundia *et al*., 1997; ATC-38, 1994). Data files that accompanied the reports listed damage to parapets as "Yes" or "No." In some cases, different types of damage (cracking, falling hazard, etc.) were listed in comment fields in the survey forms. The peak ground acceleration (PGA) for the observed locations were obtained from USGS ShakeMap. Damage descriptions were limited; thus, no differentiation was made between cracking/sliding and toppling damage. A logarithmic cumulative distribution with a median value of 0.52g PGA and a dispersion of 0.5 was the best fit through the combined data sets. The above data are plotted in Figure 3 (right) along with the fitted fragility function.

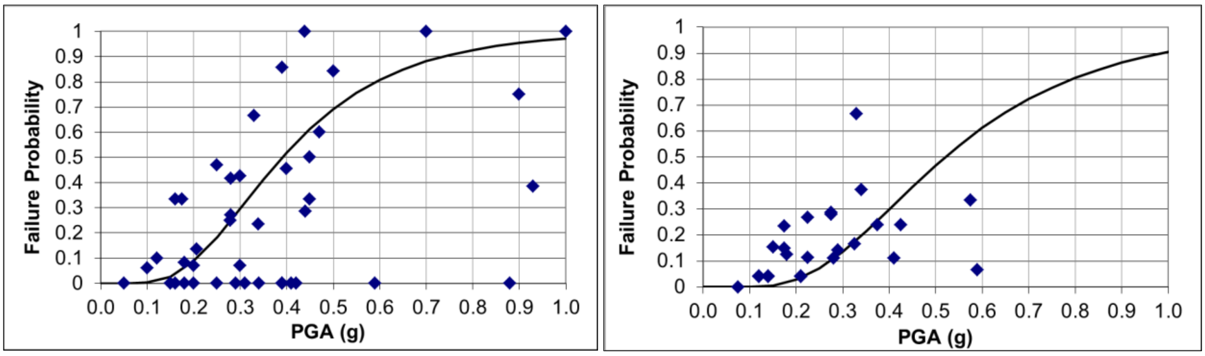

Figure 3. Fragility functions fitting empirical data for toppling of chimneys (left) and parapets (right).

3. ANALYTICAL MODELS

A basic assumption in this review is that chimneys/parapets are simple cantilever elements with negligible bending strength at the roof line and can be treated as rigid blocks that will slide and ultimately overturn as the intensity of the ground motion increases. Many analytical studies have been performed in the past 50 years on rocking and overturning of rigid blocks. An early and important study of the rocking of rigid blocks by Housner (1963) explored anomalous damage observations after several earthquakes, namely, the survival of tall slender monuments and structures in areas where their squat and apparently stable counterparts were severely damaged. Housner showed that there is a size effect, that is, the propensity for overturning is not governed solely by aspect ratio, and that dynamic survival is not predicted by simple statics.

3.1. Previous studies

Since Housner's paper there have been many researchers who have studied the response of rigid blocks; we identify a few here, but acknowledge this is by no means an exhaustive list. Aslam *et al.* (1980) carried out a series of shake table tests of rigid block rocking and showed that the response of the block was so sensitive to input parameters that experimental results using earthquake ground motions were not repeatable, much less predictable. Yim *et al*. (1980) showed though numerical simulation that while individual responses could differ, they showed that in a probabilistic sense the vulnerability to overturning increases with aspect ratio and motion intensity, and decreases with block size. Spanos and Koh (1984) defined the governing differential equations for rocking blocks and used numerical integration to show, among other things, combinations of frequency and amplitude that lead to overturning for differing block aspect ratios. More recently, Sharif *et al*. (2007) and Meisl *et al.* (2007) have investigated probabilistic failure criteria for rocking of block walls with anchorage to diaphragms.

3.2. Computer simulations with Working Model 2D

Considering the disparity of results obtained in various analytical studies on rocking of rigid blocks, and the apparent sensitivity of the results to motion frequency characteristics, the need was evident for comprehensive simulations using a set of representative ground motions. This study focused on the response evaluation of parapets using the dynamic simulation software Working Model 2D (Design Simulation Technologies, 2005). The software permits simulation of one-dimensional ground motion and representation of structures by means of rigid bodies and springs.

3.2.1. Chimney analytical model

Two types of chimneys were investigated: a free-standing chimney and a rooftop chimney attached to a building at the eave line. The free-standing chimney model is a rigid block resting on a rigid foundation. This model is a reasonable representation of older vintage chimneys, or poorly constructed modern chimneys that have suffered cracking at the base and full or partial detachment from the structure. Sliding towards the building was not allowed, that is, the chimney was only allowed to slide away from the building. The rooftop chimney consists of a rigid block resting on the edge of a building. The building is represented by a single, hinged portal frame with large mass (relative to the chimney), a lateral stiffness resulting in an undamped period of 0.1 seconds, and a dashpot that results in 5% critical damping. The top of the frame is at 120 inches above the rigid foundation, corresponding to the eave elevation of the benchmark case. The following properties of the chimney were used: width B = 24 in.; height H = 132 in., 180 in., and 228 in.; masonry unit weight = 120 lb/ft^3; coefficient of restitution = 0.02; and coefficients of static and dynamic friction = 0.8 and 0.7, respectively. The coefficient of restitution appears to be small, but it provided the best match with experimental results reported in Sharif *et al*. (2007). Sensitivity studies showed that variations of the coefficient of restitution and friction coefficients had little effect on fragility functions. The analytical models for the free-standing and rooftop chimney cases are shown in Figure 4.

Arguments for the height dimensions are as follows: Assume ground-to-top-of-eave height of 120 inches. A typical chimney extends about 60 inches above the height of the eave, resulting in a total height of 180 inches. This height is consistent with the 2006 International Residential Code (IRC), which requires a 10-foot horizontal clearance between the chimney wall and the roofing surface at an elevation 2 feet below the top of chimney. For a common 4:12 pitched roof, this would require 64-inch extension - rounded herein to 60 inches. The taller chimney variant is based on the same considerations but for a 9:12 roof slope (steep but not rare), for which the IRC would require 2+10*(9/12) = 9-feet (rounded down), for a total chimney height of 228 inches. For a lower bound chimney height, relative to the benchmark, we assumed a total chimney height of 132 inches. For the rooftop chimney, the dimension to the top of the eave was kept constant at 120 inches and the upper block was taken as 60 inches and 108 inches, respectively.

3.2.2. Parapet analytical model

The rooftop parapet is assumed to be free-standing and not structurally braced to the roof structure, appropriate assumptions for older vintage parapet walls or poorly constructed modern parapets. The parapet was modeled as a rigid block resting on the edge of a hinged portal frame that represents the lateral response at mid-span of a wood-framed diaphragm of a typical masonry building. The portal frame is connected to a rigid foundation accelerated horizontally with the set of ground motions. Similar to the rooftop chimney, the lateral stiffness and damping were modeled with an elastic spring and dashpot spanning the diagonal of the portal frame and were tuned to represent the expected behavior of common two-story commercial masonry buildings. The spring stiffness was calculated based on assumed first mode periods of T = 0.2 sec., 0.35 sec., and 0.6 sec. The following properties of the parapet were used: height x width = 36 in. x 12 in. and 24 in. x 8 in.; unit weight = 120 lb/ft^3; coefficient of restitution = 0.02; and coefficient of static and dynamic friction = 0.8 and 0.7, respectively. The damping ratio was chosen as 5% of critical. The analytical model for the parapet is shown in Figure 4 (right).

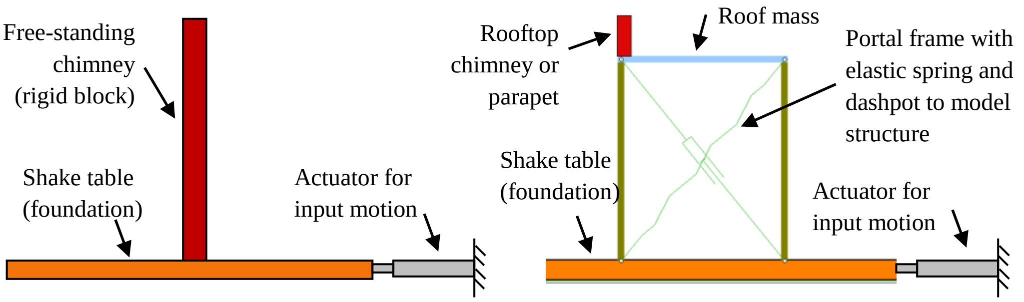

Figure 4. Computer model of free-standing chimney (left) and rooftop chimney or parapet (right).

4. ANALYTICAL RESULTS

Using Working Model 2D, each of the models was subjected to the ATC-63 (FEMA P695) set of 44 ground motion records (actually 22 pairs of records). This record set is discussed in detail in FEMA (2009). The records represent ground motions recorded at sites greater than 10km from the fault rupture. The records are intended to represent an unbiased suite of motions associated with earthquake magnitudes between 6.5 and 7.9. Incremental dynamic analysis (IDA) was performed for each record, whereby the intensity of the record was increased until “significant” sliding and then toppling of the chimney/parapet occurred. The sliding capacity was defined as that ground motion intensity that causes residual sliding of at least 1/16 in. Toppling was defined as overturning of the chimney/parapet block.

Various intensity measures (IMs) associated with the two failure modes were recorded, among them, peak ground acceleration (PGA), peak ground velocity (PGV), spectral acceleration, S_a, of the roof at T = 1 sec., S_a of the roof at the structure/diaphragm fundamental period, and Peak Total Roof Velocity (PTRV). The PTRV is the peak of the sum of the relative roof velocity (at the structure/diaphragm fundamental period) and the ground motion velocity. The analysis results were post-processed by sorting each record by the IM value at the point of failure (sliding greater than 1/16 in., or toppling). The sorted records were used to assemble the analytical cumulative distribution functions (probability of failure given IM), and lognormal distributions were fit to the CDFs using least squares.

4.1. Free-standing chimney

Figure 5 (left) shows sliding and toppling fragility functions for the average chimney height of 180 in. The median sliding capacity for the free-standing chimney is only about 20% smaller than the toppling capacity. From the perspective of repair, the two damage states are essentially identical (assuming no consequential physical damage for the toppling state: removal and replacement of the chimney above the crack. The significant distinction between sliding and toppling is the life safety concern associated with toppling. The effect of chimney height on toppling fragility functions is shown in Figure 5 (right). For the range of heights considered for the free-standing chimney, the effect of different chimney heights is relatively small and can be accounted for by increasing the dispersion β by a small amount.

Based on the analytical results obtained here, and considering the uncertainties in the assumptions made for sliding and rocking of rigid blocks, a median toppling capacity of 0.5g with a β of 0.6 is recommended. The results indicate a median sliding capacity of 0.4g with a β less than 0.5. These values apply for free-standing, non-engineered (without reliable reinforcement) chimneys that are not attached to the building and not affected by the motions of the building. It is reasonable to use the same values for non-engineered chimneys that are nominally attached to the building, but with an attachment that does not provide sufficient resistance to prevent sliding or rocking.

4.2. Rooftop chimney

In this simulation it is assumed that the chimney attachment to the building is of sufficient strength and stiffness so that no relative translation can take place between the chimney and the building. Thus, toppling and sliding can occur only at the eave level. This model captures damage related to the portion of the chimney extending above the roof line (perhaps the most common damage mode).

Toppling fragility functions are presented in Figure 6 (right) for “rooftop” chimneys extending 60 in. and 108 in. above the eave line, together with the fragility function for the free-standing 180 in. chimney. The attachment to the building causes a clear increase in median toppling capacity, but the increase depends strongly on the height of the chimney above the eave line. If this height is 60 in. (which results in a total chimney height of 180 in. if the eave height is 120 in.), the increase is about 60% compared to the free-standing chimney, but it is only about 25% if the height above the eave is 108 in.

The sliding fragilities shown in Figure 6 (left) indicate that sliding occurs at a lower PGA for an attached (or rooftop) chimney than for a free-standing chimney, and that the capacity is sensitive to the height of the chimney block above the roof line. For this reason it is recommended to reduce the median sliding capacity for non-engineered chimneys from the value of 0.4g recommended for free-standing chimneys to a value of 0.35g and to increase the dispersion β to 0.6. The observation that the sliding capacity for a rooftop chimney decreases compared to a free-standing chimney is not surprising, because the maximum input acceleration imparted by the building to the rooftop portion of the chimney increases greatly compared to the PGA and overcomes the beneficial effect of a smaller aspect (H/B) ratio. The higher acceleration will cause early uplift, which in turn will cause early bouncing and sliding. This is much more evident in the 108-inch tall rooftop chimney block (H/B = 4.5) than the 60-inch block (H/B = 2.5). A mitigating condition is that for large PGAs the building is expected to respond inelastically, and very high roof accelerations are not very likely to develop. The final, proposed fragilities for non-engineered chimneys (considering both free-standing and rooftop cases) are shown in Figure 7.

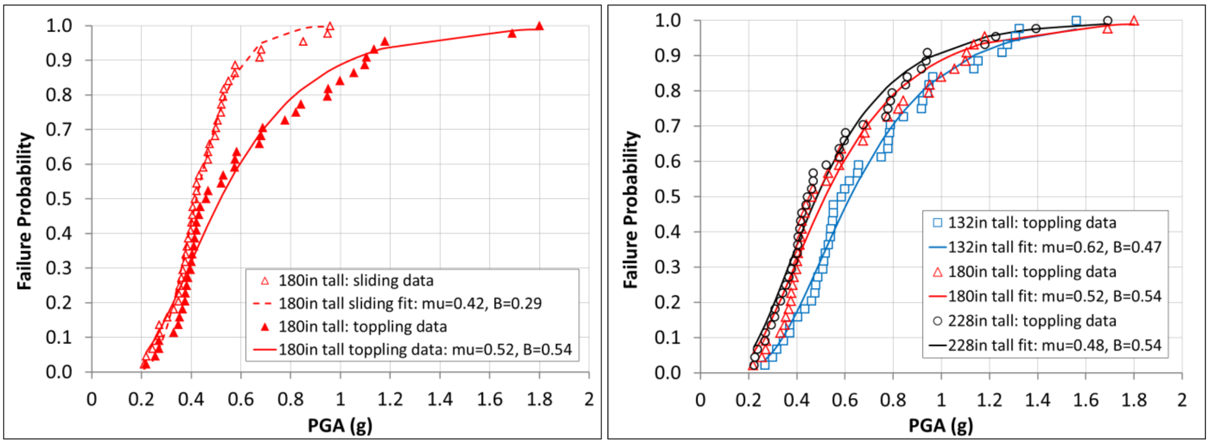

Figure 5. Sliding and toppling fragilities for 180 in. tall free-standing chimney (left) and toppling fragilities for free-standing chimneys of different heights (right).

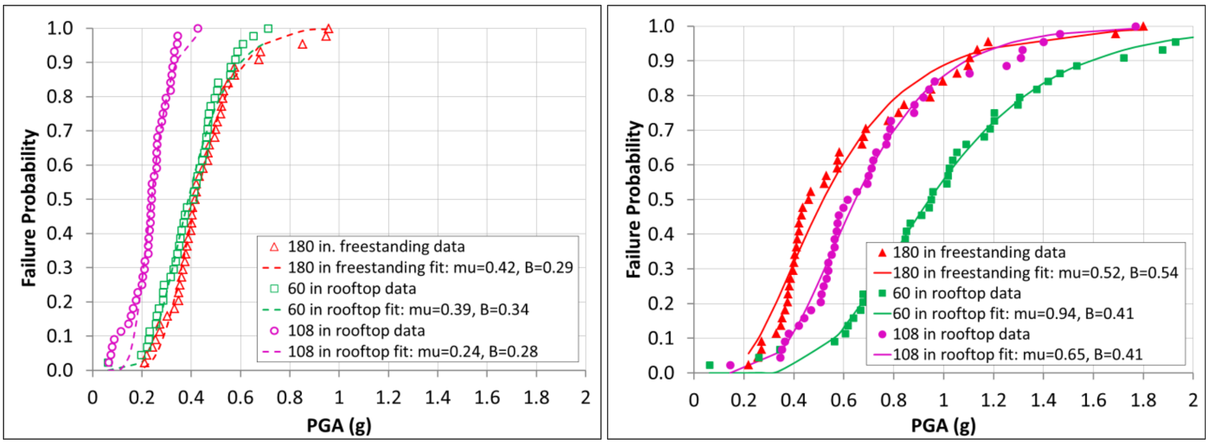

Figure 6. Sliding fragilities for rooftop chimneys (left) and toppling fragilities for rooftop chimneys (right). Freestanding fragilities for the 180-inch tall chimney is shown for reference.

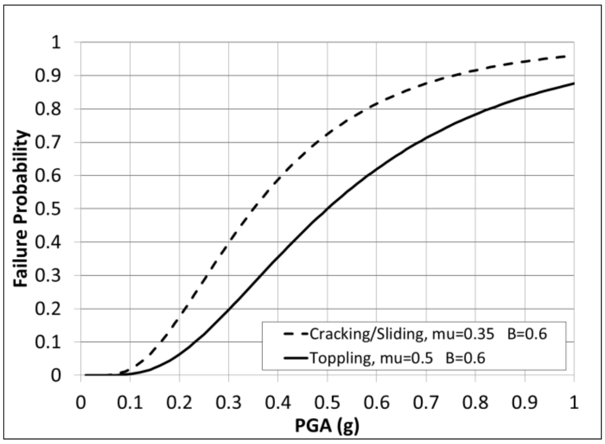

Figure 7. Proposed chimney fragility functions with PGA as seismic intensity measure.

4.3. Parapet

The parapet model was analyzed for both a 36-inch tall by 12-inch wide parapet and a 24 in. by 8 in. parapet. The differences between the two parapet sizes are small, with an increase in capacity for the 24 in. by 8 in. parapet of only about 10%. Thus, all fragilities presented herein are for the 36 in. by 12 in. parapet.

Fragilities for the two parapet damage states were generated for several IMs and diaphragm/structure periods. For example, fragilities are shown in Figure 8 for the parapet model with a diaphragm/ structure period of T=0.2 sec. and PGA and Peak Total Roof Velocity (PTRV) as intensity measures. The median values for sliding and toppling capacity are about 0.17g PGA and 0.44g PGA, respectively. These values depend strongly on the period of the structure/diaphragm system on which the parapet rests, and on the parapet aspect ratio. In the case of Figure 8, T = 0.2 sec. was used, corresponding to the peak in the spectral acceleration plot of the selected ground motion set. At this period the spectral amplification of the PGA for the selected ground motion set is about 2.5. For shorter and longer periods the amplification will be smaller. For smaller parapet aspect ratios the median capacities are expected to slightly increase. Moreover, no credit is given in this analysis to restraining effect provided by plate action of the parapet. For these reasons an increase in median capacities appears to be justified. Considering the wide range of parapet aspect ratios and boundary conditions, and particularly the large uncertainty in the period of the structure/diaphragm on which the parapet rests, a large dispersion is appropriate, i.e. $\beta = 0.6$. The final, proposed fragility functions for several intensity measures and diaphragm/structure periods are shown in Figure 9.

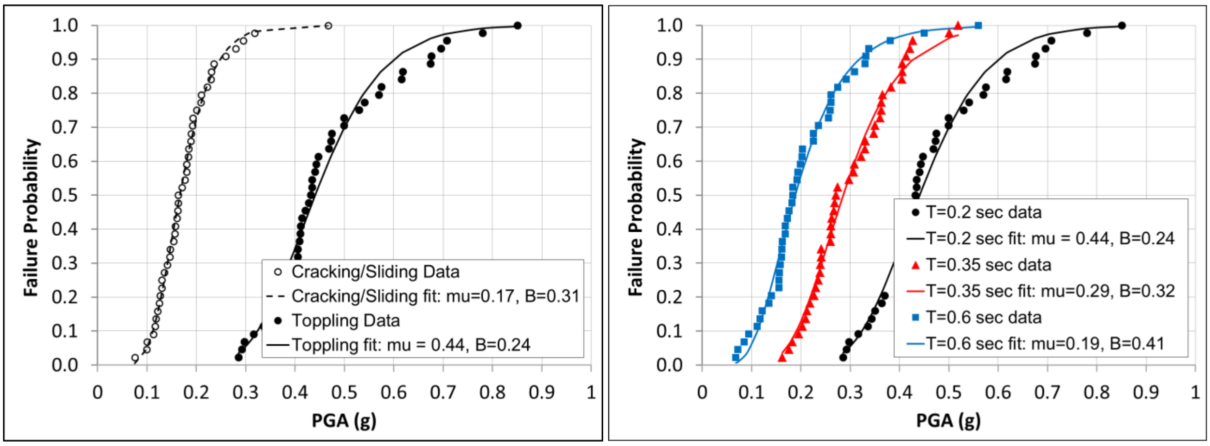

Figure 8. Sliding and toppling fragilities for parapet with diaphragm/structure period of T=0.2 sec. (left) and toppling fragilities for parapets with different diaphragm/structure periods (right).

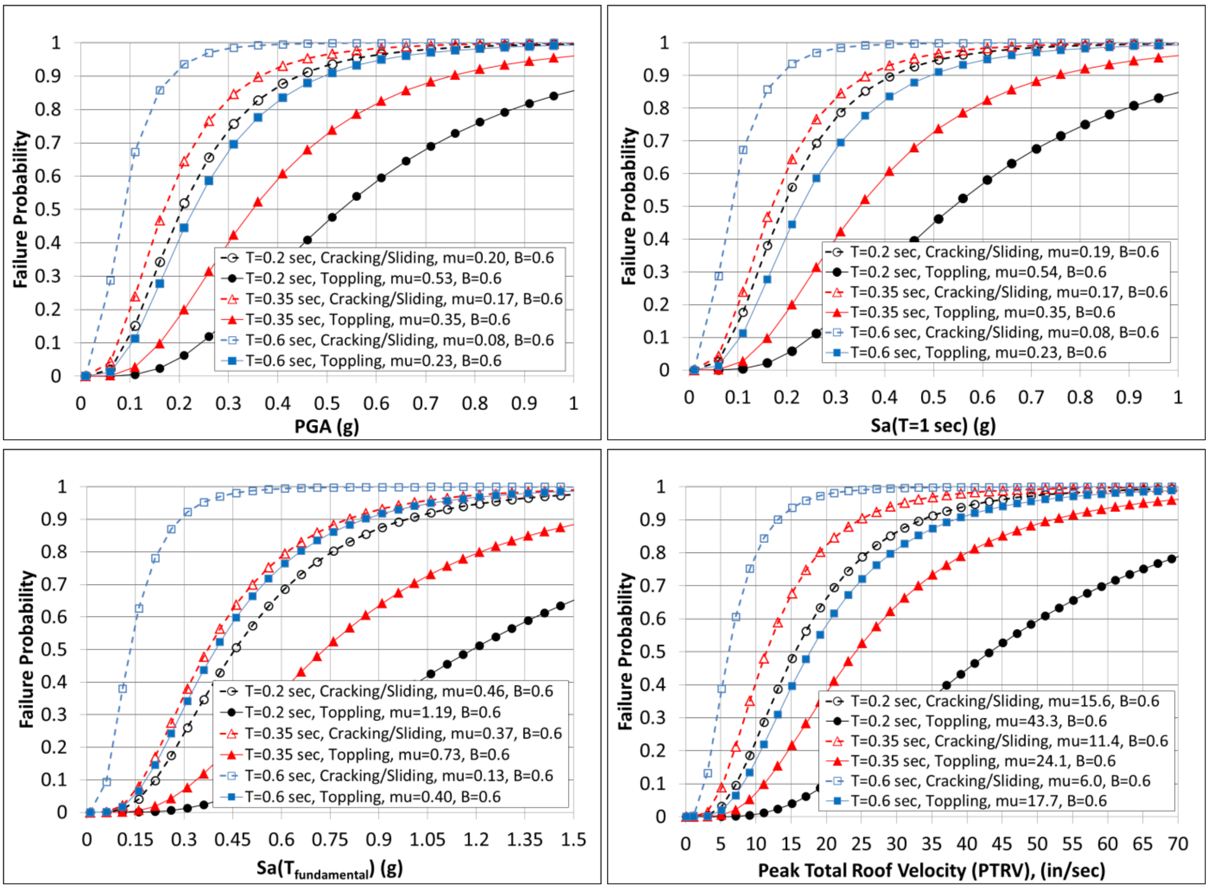

Figure 9. Proposed parapet fragility functions for different seismic intensity measures and diaphragm periods.

5. CONCLUSIONS

Masonry chimneys and parapets are two of the most fragile building components, and they are consistently damaged in earthquakes. In fact, damage states of masonry chimneys/parapets after earthquakes are one of the intensity measures used to assess the Modified Mercalli Intensity (MMI) in an area. Several sets of post-earthquake field reports and damage surveys were analyzed to develop empirical fragility functions. In addition, chimney/parapet response was investigated with computer simulations using incremental dynamic analyses. After considerable effort to develop fragility functions using either empirical data or analytical studies, it was concluded that neither approach would provide defensible fragility functions. Rather, the final, proposed fragility functions (Figure 7 and Figure 9) were derived using a hybrid approach, based on the insight gained from analysis of empirical data and numerical simulation of chimney/parapet response.

AKCNOWLEDGEMENTS

Professor Helmut Krawinkler, leader of this study, passed away April 16, 2012. Helmut provided a life-time of wisdom, insight, and gentle mentorship to the junior authors. His contributions to this work, the engineering profession, and our lives cannot be overstated. He is deeply missed.

This paper is based upon work supported by the ATC-58 Project "Guidelines for Seismic Performance Assessment of Buildings." Any opinions, findings, and conclusions or recommendations herein are those of the authors and do not necessarily reflect those of the sponsors.

REFERENCES

Aslam M.; Godden, W.G.; and Scalise, D.T. (1980). Earthquake Rocking Response of Rigid Bodies, Journal of the Structural Division – Proceedings of the American Society of Civil Engineers, Vol. 106, No. 2, February, pp. 377-392.

ATC-38 (2001). Database on the performance of structures near strong-motion recordings: 1994 Northridge California Earthquake, Applied Technology Council.

Baker and Zareian (2009). Maximum Likelihood routine for fitting log-normal curves, personal comm. with H. Krawinkler.

Booth, D.B.; Wells, R.E.; and Givler, R.W. (2004). Chimney Damage in the Greater Seattle Area from the Nisqually Earthquake of 28 February 2001, BSSA Vol. 94 No. 3, June, pp. 1143-1158.

CEA (2009). San Simeon Earthquake chimney data, personal comm. between Dan Dyce and J.D. Osteraas.

Design Simulation Technologies, Inc (2005). Working Model 2-D 2005, http://workingmodel.design-simulation.com/WM2D/index.php

FEMA (2009). Quantification of Building Seismic Performance Factors, FEMA P-695 Report, prepared by the Applied Technology Council for the Federal Emergency Management Agency, Washington, D.C.

Graf, W.P. (2009). 1994 Northridge Earthquake chimney damage data, personal comm. with J.D. Osteraas.

Griffith, M.; Ingham, J.; and Moon, L. Implications of the 2010 Darfield (Christchurch, NZ) earthquake for Australia – are we ready?, Proceedings of the Australian Earthquake Engineering Society 2010 Conference, Perth, Western Australia, Paper No. 55.

Housner, G.W. (1963). The Behavior of Inverted Pendulum Structures During Earthquakes, Bulletin of the Seismological Society of America, Vol. 53, No. 2, February, pp. 403-417.

LADB&S (1994). Northridge Earthquake Repair Permit Database, LA Department of Building and Safety.

Lizundia, B., et. al. (1991). Damage to Unreinforced Masonry Buildings in the October 17, 1989 Loma Prieta Earthquake, Technical Report to NSF and California Seismic Safety Commission, February.

Lizundia, B.; Holmes, W.T.; Longstreth, M.; and Kren, A. (1997). Development of Procedures to Enhance the Performance of Rehabilitated URM Buildings (with Appendices), National Institute of Standards and Technology, Report NIST GCR 97-724-1 and 97-724-2, August.

McMullin K.M.; Garvey, T.; and Parrott, S. (2001). The February 28, 2001 Nisqually Earthquake: Reconnaissance Report, Collaborative for Disaster Mitigation, Report CDM/2001/01, San Jose State University Foundation, April 25.

Meisl C.S.; Elwood K.J.; and Ventura C.E. (2007). Shake Table Tests on the Out-of-Plane Response of Unreinforced Masonry Walls, Canadian Journal of Civil Engineering, Vol. 34, No. 11, pp. 1381-1392.

Newstalk ZB (2010). "Most damage claims over $10k", http://www.newstalkzb.co.nz/newsdetail1.asp?storyid=182291, Sept. 13, 2010. Retrieved 13 Sept 2010.

Scholl, R.E. (1974). Statistical Analysis of Low-rise Building Damage Caused by the San Fernando Earthquake, BSSA Vol. 64, No. 1, pp. 1-23.

Sharif, I.; Meisl C.S.; and Elwood K.J. (2007). Assessment of ASCE 41 Height-to-Thickness Ratio Limits for URM Walls, Earthquake Spectra, Vol. 23, No. 4, November, pp. 893-908.

Spanos P.D. and Koh A.S. (1984). Rocking of Rigid Blocks Due to Harmonic Shaking, Journal of Engineering Mechanics, Vol. 110, No. 11, November, pp. 1627-1642.

Yim, C.S.; Chopra A.K.; and Penzien, J. (1980). Rocking Response of Rigid Blocks to Earthquakes, Earthquake Engineering and Structural Dynamics, Vol. 8, pp. 565-587.